A Model of Composite Propellant Combustion Including Surface Heterogeneity and Heat Generation

CLARKE E. HERMANCE*
University of Waterloo, Waterloo, Ontario, Canada

The surface heterogeneity of a composite propellant is incorporated in a model of the propellant combustion process. This process is pictured as the sum of fuel pyrolysis, oxidizer decomposition, heterogeneous chemical reaction between the fuel and decomposed oxidizer in small fissures surrounding individual oxidizer particles, and gas phase combustion of all final decomposition products. Expressions for the burning rate and the rate of heat generation at the propellant surface and in the gas phase flame are formulated, explicitly including the oxidizer particle size distribution. Expressions for the mean, one-dimensional, propellant surface and flame temperatures are derived assuming planar regions of heat generation. A collected set of implicit, algebraic equations is solved numerically for the propellant burning rate, surface (and flame) temperatures for a variety of physical parameters. The burning rate is found to depend strongly on the oxidizer particle ignition delay at low pressures, and upon the position of the external flame at high pressures. The effect of the heterogeneous reaction on the burning rate is strongest at intermediate pressures. The results agree quite well with experimental data on the effect of pressure and oxidizer particle size on composite propellant burning rates, surface temperatures, and surface structure.

Nomenclature

A = mass of fuel vapor released by pyrolysis, g [see Eq. (1)]
A_f = pre-exponential factor for fuel binder pyrolysis, cm/sec
B = mass of fuel vapor produced by oxidizer decomposition, g [see Eq. (2)]
(B) = mass concentration of B, g/cm^3
C = mass of oxidant vapor produced by oxidizer decomposition, g [see Eq. (2)] and identified as $HClO_4$ when oxidizer is NH_4ClO_4
(C) = mass concentration of C, g/cm^3
c = specific heat of solid propellant, 0.4 cal/g-°K
c_p = constant pressure specific heat of combustion gases, 0.3 cal/g-°K
D_1, D_2 = mass of reduced oxidizer vapors produced by surface and gas phase reactions, g [see eqs. (3) and (4)]
D, D_i = diameter of oxidizer crystals, μ
ΔD_1, ΔD_2 = number of integer diameters between maximum and minimum diameters of respective oxidizer particle size distributions
D_c = characteristic diameter of decomposing oxidizer crystal, μ [see Eq. (13)]
E_f, E_{sr}, E = activation energies of fuel binder pyrolysis, surface reaction, and gas phase reaction, respectively (kcal/mole)
E_{ox} = half the activation energy of the oxidizer decomposition (~56 kcal/mole for NH_4ClO_4)
g = acceleration of gravity, taken as 980 cm/sec^2
ΔH_y = endothermic heat of pyrolysis, cal/g
J = mechanical equivalent of heat, 4.185×10^7 erg/cal
Ko = oxidizer ignition delay parameter, sec-(atm)^m-(cm)$^{-n+1}$ (k of Ref. 8)
k_f, k_{ox} = mass flow rates in g/sec of fuel pyrolysis and oxidizer decomposition
k_{sr}, k_{sr}' = rate constants associated with surface reaction, cm^3/sec and cm/sec, respectively
M_g, M_c = molecular weight of combustion gases and C, respectively
M_i, m_i = mass flow rate, mass flux, associated with propellant component as designated by subscript, g/sec and g/cm^2 sec, respectively
m = diameter exponent in particle ignition term [see Eq. (12)]
n = pressure exponent in particle ignition term [see Eq. (12)]
P = ambient pressure, atm
P_c = partial pressure of oxidant C, g$_f$/cm^2
P_1, P_2 = mass of inert products, or oxidized fuel vapors produced by gas phase reactions, g [see Eqs. (3) and (4)]
Q_L = latent heat of oxidizer decomposition
Q_{gp} = gas phase heat release of oxidizer decomposition
Q_{sr} = heat released by surface reaction, cal/g
Q_f = heat released in gas phase flame of propellant, cal/g
r = propellant burning rate, cm/sec
R = gas constant, 1.986 cal/mole-°K
S_f = surface area of fuel pyrolysis, cm^2
S_{ox} = planar surface area of oxidizer decomposition, cm^2
S_{sr} = surface area available for surface reaction, cm^2
S_0 = total planar, cross-sectional area of burning surface of propellant, cm^2
T, T_p = temperature, and propellant initial temperature, °K
t_c = characteristic time of exposure of oxidizer crystal at propellant surface [see Eq. (14a)]
t_{ign} = ignition delay time of oxidizer crystal, sec
v_b = linear burning rate of an oxidizer crystal, cm/sec
V = linear burning rate constant of oxidizer crystal, cm-sec^{-1} atm$^{(-\delta)}$
x^* = flame standoff distance, cm
Z = pre-exponential factor of gas reaction rate, cm^3/g-sec
α = weight fraction of oxidizer in propellant
β = $(c_p/\lambda_g Z)(\rho_p J/1033.gM_g)^2$, const
λ_g = thermal conductivity of combustion gases, 2×10^{-4} cal/cm-sec-°K
ν = volume fraction of oxidizer in propellant
ρ = density, g/cm^3
σ = fraction of oxidizer having particle size spread ΔD_2
θ = dimensionless temperature, RT/E
ξ = $(m_T c_p/\lambda_g)X$, dimensionless length
ϵ = depth of fissure surrounding oxidizer crystals
δ = pressure exponent of oxidizer burning rate

Presented as Preprint 66-112 at the AIAA 3rd Aerospace Sciences Meeting, New York, January 24–26, 1966; submitted January 27, 1966; revision received June 6, 1966. This work was sponsored by The Aeronautical Research Institute of Sweden (FFA), Bromma, Sweden, in cooperation with The Swedish Institute for Defense Research (FOA), Stockholm, Sweden. The author wishes to express his appreciation to G. Drougge, Director of Research, FFA, and T. Marklund, Director of Solid Propellant Research, FOA, for the opportunity of cooperating with their institutes in Sweden. Particular thanks are due T. Marklund for his interest and many stimulating discussions with regard to this work.

* Assistant Professor, Department of Mechanical Engineering. Member AIAA.

Subscripts

p = propellant
s = surface
sr = surface reaction
ox = oxidizer
T = total
gp = gas phase
L = latent
f = fuel, flame
c = oxidant vapor C

Numerical constants

$c_1 = 1.36\,(3637.7)(g/J)\exp(24.38)$
$c_2 = (24)^{1/2} \cdot C_1$
$c_3 = 0.5(1 + 3^{-1/2})$
$a_1 = [(1 - \nu)/(1 - \alpha)]\rho_f A_f/\rho_p$
$a_2 = a_1(1 - \alpha) \cdot \Delta H_p R/c_p E$
$a_3 = Q_f R/c_p E$
$b_1 = (c_2 M_c \nu V)/[\rho_p(1 - \alpha)(REM_g)^{1/2}]$
$b_2 = (c/c_p)\,\theta_p + \alpha(Q_{gp} - Q_L)R/c_p E$
$b_3 = b_1(1 - \alpha)(Q_{sr} - Q_{gp})R/c_p E$

$$d_1 = K_0\left[\left(\frac{1-\sigma}{\Delta D_1 + 1}\right)\sum_{i=1}^{\Delta D_1+1} D_i{}^n + \left(\frac{\sigma}{\Delta D_2 + 1}\right) \times \sum_{i=1}^{\Delta D_2+1} D_i{}^n\right]$$

Introduction

DURING the development and use of composite solid propellants, several theories concerning the combustion mechanism of these propellants have been presented. The theories have ranged from detailed treatments of oxidizer and fuel decomposition in a "sandwich" propellant,[1] to the broad treatment incorporated in the "granular diffusion flame" model.[2] Although useful in helping to quide experiments to gather information about the combustion process of composite propellants, it is not unfair to note that these theories have had limited success in explaining or predicting many features of composite propellant combustion which are evident in the extensive experimental data available. Perhaps the most striking features of these data are 1) the effect of different fuel binders on the burning rate-pressure relationship[3]; 2) the variation of the burning rate pressure exponent with ambient pressure level, particularly the near unity values of this exponent at pressures in the region of 4000 psia[3]; 3) the dependence of the burning rate on the oxidizer particle size distribution and the disappearance of particle size effects at high pressures[4]; 4) the value of the mean surface temperature of the burning propellant and the possible insensitivity of this temperature to ambient pressure level[5]; 5) the evidence of a substantial energy release at, or very close adjacent to, the propellant surface.[2,5]

The purpose of the present paper is to describe a model of composite propellant combustion which incorporates the heterogeneity of the burning surface of composite propellants caused by the oxidizer particles, and a mechanism for substantial energy release at the burning surface, in an attempt to account theoretically for the aforementioned features of composite propellant combustion.

It must be emphasized at this point that, although the following theory is tested with respect to ammonium perchlorate propellants, the formulation is such that any composite propellant can be considered providing appropriate data on the individual components is available.

Description of Model

The physical-chemical processes incorporated in the model are the surface processes of endothermic fuel binder pyrolysis, exothermic oxidizer decomposition, exothermic heterogeneous chemical reaction between the fuel binder and decomposed oxidizer in small regions surrounding individual oxidizer particles, and the gas phase process of combustion of the final fuel and oxidizer decomposition products. Each of these processes depends on either, or both, the ambient pressure level and the temperature present at the location of the process in question; they are linked together by the temperature distributions present in the gas and solid phases. Evidently the temperature distribution depends on the interaction of the heat source (or sink) at the propellant surface, and the heat source in the gas phase caused by the final combustion process. The magnitudes of these heat sources are determined by the details of the respective surface and gas phase processes. The proposed structure of these processes follows, assuming that all undecomposed oxidizer crystals are spherical.

Surface Processes and the Burning Rate

The over-all burning rate of a composite propellant should be determined ultimately by the sum of the decomposition rates of the propellant components. It is postulated that these decomposition processes can be represented by the following reaction sequence, where S stands for surface and k_i denotes the mass production rate of the reaction:

a) Fuel binder decomposition by pyrolysis

$$S_f \xrightarrow{k_f} A - \Delta H_p \tag{1}$$

b) Initial decomposition step of the oxidizer

$$S_{ox} \xrightarrow{k_{ox}} B + C - Q_L \tag{2}$$

c) Heterogeneous reaction between oxidant C from Eq. (2) and the fuel binder to produce products, a reduced oxidizer, and heat

$$C + S_{sr} \xrightarrow{k_{sr}} P_1 + D_1 + Q_{sr} \tag{3}$$

d) Second decomposition step of oxidizer, close to the oxidizer crystal producing heat, a reduced oxidizer, and other inerts and combustibles†

$$B + C \xrightarrow{k_{gp}} P_2 + D_2 + Q_{gp} \tag{4}$$

Adopting the methods of chemical kinetics, the total mass flow away from the propellant surface is given by

$$M_T = A_t + B_t + C_t + (P_1 + D_1)_t + (P_2 + D_2)_t \tag{5}$$

where

$$\begin{aligned} A_t &= k_f \\ B_t &= \tfrac{1}{2}k_{ox} - k_{gp}(B)(C) \\ C_t &= \tfrac{1}{2}k_{ox} - [k_{sr}(C) + k_{gp}(B)(C)] \\ (P_1 + D_1)_t &= 2k_{sr}(C) \\ (P_2 + D_2)_t &= 2k_{gp}(B)(C) \end{aligned} \tag{6}$$

Under the postulate $C_t = 0$, or there is no net flow of reactive oxidant C‡ away from the propellant surface, the total mass flow away from the propellant burning surface is given by

$$M_T = k_f + k_{ox} + k_{sr}(C) \qquad \text{g/sec} \tag{7}$$

To derive an expression for the burning rate, it is only necessary to note that

$$m_T = \rho_p r = M_T/S_0 = k_f/S_0 + k_{ox}/S_0 + k_{sr}(C)/S_0 \tag{8}$$

† The production of a reduced oxidizer in step d is necessary for the existence of an external, gas phase flame.

‡ For the ammonium perchlorate propellants dealt with in the numerical calculations of this paper, C is identified as $HClO_4$ (perchloric acid) an oxidizer that can support combustion.[6]

where

$$k_f = m_f S_f \qquad k_{ox} = m_{ox} S_{ox}$$
$$k_{sr}(C) = m_{sr} S_{sr} = k_{sr}'(C) \cdot S_{sr} \tag{9}$$

such that

$$r = 1/\rho_p [m_f(S_f/S_0) + m_{ox}(S_{ox}/S_0) + m_{sr}(S_{sr}/S_0)] \tag{10}$$

Consequently, it is necessary to calculate the area ratios in the preceding equation.

Calculation of Mass Flux Area Ratios

Assuming that the mean fuel surface, i.e., between oxidizer crystals on the propellant burning surface, is planar, and a total volume fraction (ν) of spherical oxidizer crystals, (S_f/S_0) and (S_{ox}/S_0) are defined as ($1 - \nu$) and (ν), respectively. The area on which the surface reaction occurs, S_{sr}, is calculated by noting that an oxidizer crystal on the burning surface should, in general, have decreased in dimension from its original size. It is postulated that the result of this dimension change is to produce a fissure of depth (ϵ) between the crystal and the fuel binder originally surrounding the crystal as sketched in Fig. 1. The area of this fissure will be taken as ($\pi D_i' \epsilon_i$) where D_i' is the chord length of an undecomposed crystal at the level of the planar fuel surface; this is the area on which the postulated surface reaction occurs.

For N_i, such spheres occupying a volume fraction ν_i, the total surface reaction area is $(S_{sr})_i = \pi(N_i D_i' \epsilon_i)$. But for a planar, cross-sectional propellant surface area S_0, it may be shown that the expected value of D_i' is $(\frac{2}{3})^{1/2} D_i$, and

$$N_i = 6\nu S_0/\pi D_i^2$$

Consequently,

$$(S_{sr}/S_0)_i = (24)^{1/2} \nu_i (\epsilon_i/D_i) \tag{11}$$

Consider a bimodal propellant, having two rectangular distributions of discrete particle diameters ΔD_1 and ΔD_2 such that the total weight fraction of oxidizer is α and the weight fraction of the total oxidizer weight of ΔD_2 distribution is σ. In such a case, a simple extension of Eq. (11) shows that the ratio (S_{sr}/S_0) is

$$\left(\frac{S_{sr}}{S_0}\right) = \nu(24)^{1/2} \left[\left(\frac{1-\sigma}{\Delta D_i + 1}\right) \sum_{i=1}^{\Delta D_1 + 1} \left(\frac{\epsilon_i}{D_i}\right) + \left(\frac{\sigma}{\Delta D_2 + 1}\right) \sum_{i=1}^{\Delta D_2 + 1} \left(\frac{\epsilon_i}{D_i}\right)\right] \tag{12}$$

wherein it is assumed that all particles have a discrete diameter of $(D_i \pm \frac{1}{2})\mu$ which is termed D_i. For the calculations resulting in Eq. (12), it is assumed that the distribution function gives "the fraction of particles, by weight, having a diameter less than D," and has shape in the form of a staircase having square steps.

Calculation of the Fissure, Depth (ϵ)

Referring to Fig. 1, it is assumed that the characteristic value of the fissure depth (ϵ_i) is given by the difference between the original value of the diameter D_i and the characteristic D_c of the decomposing crystal. The value of D_c is given by

$$D_c = D_i - v_b(t_c - t_{ign}) \tag{13}$$

where (v_b) is the linear regression rate of the oxidizer at the particular ambient pressure level; t_{ign} is the ignition delay of the individual crystal, assuming the ignition process starts when the top of the crystal becomes just tangent to the planar fuel surface. The characteristic time t_c is the time necessary for the burning surface to regress the distance L from the top of the crystal to a position such that the diameter of

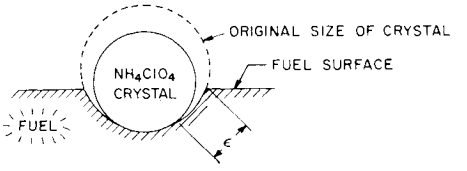

Fig. 1. Sketch showing reaction depth around on oxidizer crystal.

crystal, at its intersection with the burning surface, is the expected value of $(\frac{2}{3})^{1/2} D_i$, or

$$L = 0.5(1 + 3^{-1/2}) D_i$$

Therefore,

$$t_c = L/r = c_3 D_i/r \tag{14a}$$

and

$$\epsilon_i = D_i - D_c = v_b(t_c - t_{ign}) \tag{14b}$$

The ignition delay and linear burning rate of ammonium perchlorate crystals have the form[7-9]

$$t_{ign} = (K_0 D_i^{n+1}/P^m) \qquad v_b = VP^\delta \tag{14c}$$

Consequently, the expression for (ϵ_i/D_i) appearing in Eq. (12) is

$$(\epsilon_i/D_i) = VP^\delta [(C_3/r) = (K_0 D_i^n/P^m)] \tag{15}$$

Substitution of Eq. (12) into Eq. (10) gives the following expression for the ratio of surface reaction area to total surface:

$$\left(\frac{S_{sr}}{S_0}\right) = \nu(24)^{1/2} VP^\delta \left\{\frac{c_3}{r} - \left(\frac{K_0}{P^m}\right)\left[\left(\frac{1-\sigma}{\Delta D_1 + 1}\right) \times \sum_{i=1}^{\Delta D_1 + 1} D_i^n + \left(\frac{\sigma}{\Delta D_2 + 1}\right) \sum_{i=1}^{\Delta D_2 + 1} D_i^n\right]\right\} \tag{16a}$$

or, for simplicity,

$$(S_{sr}/S_0) = \nu(24)^{1/2} \langle \epsilon/D \rangle \tag{16b}$$

Final Expression for Burning Rate

In the expression derived for the propellant burning rate [Eq. (10)], the terms m_f, m_{ox}, and m_{sr} are the mass fluxes caused by the processes of fuel pyrolysis, ammonium perchlorate decomposition, and the heterogeneous chemical reaction between the solid fuel and gaseous oxidant produced by the oxidizer decomposition.

The mass flux caused by fuel pyrolysis is taken to be of the form

$$m_f = \rho_f A_f \exp(-E_f/RT_s) \tag{17}$$

With regard to the oxidizer mass flux, the over-all propellant formulation must be preserved, which results in the relationship,

$$m_{ox} = (\alpha/\nu) m_T \tag{18}$$

The calculation of the mass flux because of heterogeneous reaction, m_{sr}, is less simple. In the derivation of Eq. (10), it should be recalled that $m_{sr} = k_{sr}' \cdot (C)$ where (C) is the concentration of gaseous oxidant and k_{sr}' is the rate constant of the reaction. This rate constant is[10]

$$k_{sr}' = \alpha \dot{c}/4 \tag{19}$$

Assuming that the sticking probability α can be represented by an Arrhenius relationship, and using the standard expression for the mean molecular velocity $\dot{c}$, the rate constant is written in the form

$$k_{sr}' = 3637.7(T_s/M_g)^{1/2} \exp(-E_{sr}/RT_s) \tag{20}$$

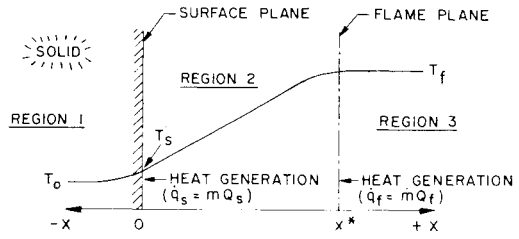

Fig. 2. Sketch of the one-dimensional model used to calculate the gas and solid phase temperature distributions.

The foregoing is approximately the value of the rate constant for the heterogeneous reaction of carbon and oxygen.[11]

Assuming ammonium perchlorate as the propellant oxidizer, (C) becomes the weight concentration of $HClO_4$. There seems to be adequate evidence that the decomposition of the ammonium perchlorate is an equilibrium process,[12] with a known equilibrium constant.[13] Therefore, the concentration of $HClO_4$, as a function of the temperature of the perchlorate crystal, is

$$(C) = M_c P_c / R_c T_s \qquad \text{g/cm}^3 \tag{21}$$

where the value of the equilibrium partial pressure of $HClO_4$, P_c, is given by

$$P_c = [1.36 \exp(24.38)] \exp(-E_{ox}/RT_s) \tag{22}$$

After condensation of the numerical constants, the mass flow rate caused by the surface reation is given by

$$m_{sr} = c_1 \left(\frac{T_s}{M_g}\right)^{1/2} \left(\frac{M_c}{R_c T_s}\right) \exp\left[\frac{-(E_{ox} + E_{sr})}{RT_s}\right] \tag{23}$$

For other oxidizers, m_{sr} should have the same general form as Eq. (23).

Equations (16a, 17, 18, and 23) can be inserted now into Eq. (10) to obtain the equation for the burning rate in terms of the surface temperature and the ambient pressure level. After collecting terms, condensing the numerical constants and using the dimensionless temperature $\theta = RT/E$, the resulting equation is

$$r = a_i \exp\left(\frac{-E_f}{E\theta_s}\right) + b_1 P^{\delta} \theta_s^{-1/2} \times \left[\left(\frac{c_3}{r}\right) - \left(\frac{d_1}{P^m}\right)\right] \exp\left[\frac{-(E_{ox} + E_{sr})}{E\theta_s}\right] \tag{24}$$

Determination of Surface and Flame Temperatures

In the derivation of the equation for the burning rate, a mean surface temperature was used; and it was implied that this temperature was uniform over the entire propellant surface. For consistency then, the surface and flame temperatures are calculated from a one-dimensional model, in which both the surface region and the gas phase flame zone are collapsed to planes where heat release takes place (see Fig. 2). The plane ($x = 0$) is assumed to remain at the surface of the propellant, and the flame position ($x = x^*$) is assumed to be a known function of the burning rate. Upon assuming a steady state, constant material properties, and unspecified but constant values of the heat released at the surface and at the gas phase flame, the following energy equations describe the temperature profiles in the regions shown in Fig. 2:

$$\begin{aligned} &\text{Region 1} && m_T c(dT_1/dx) = \lambda_p(d^2T_1/dx^2) \\ &\text{Region 2} && m_T c_p(dT_2/dx) = \lambda_g(d^2T_2/dx^2) \\ &\text{Region 3} && m_T c_p(dT_3/dx) = \lambda_g(d^2T_3/dx^2) \end{aligned} \tag{25}$$

These equations are subject to the following boundary conditions:

$$\begin{aligned} &x \to (-\infty): && T_1 \to T_p \\ &x = 0: && -\lambda_p(dT_i/dx) + m_T c T_1 + m_T Q_s = \\ & && -\lambda_g(dT_2/dx) + m_T c_p T_2; \quad T_1 = T_2 \\ &x = x^*: && -\lambda_g(dT_2/dx) + m_T c_p T_2 + m_T Q_f = \\ & && -\lambda_g(dT_3/dx) + m_T c_p T_3; \quad T_2 = T_3 \\ &x \to (+\infty): && T_3 \text{ finite} \end{aligned} \tag{26}$$

Using the dimensionless temperature, $\theta = RT/E$, and the dimensionless length, $\xi = (m_T C_p/\lambda_g)x$, this set of equations can be solved to give the following the dimensionless surface and flame temperatures:

$$\theta_s = (c/c_p)\theta_p + (Q_s R/c_p E) + (Q_f R/c_p E) \exp(-\xi^*) \tag{27}$$

$$\theta_f = \theta_s + (Q_f R/c_p E)[1 - \exp(-\xi^*)] \tag{28}$$

The heat released in the flame Q_f will be taken as a known constant for a given propellant and will be independent of the burning rate or pressure. However, the surface heat release Q_s and the flame standoff distance ξ^* are not necessarily constant and must be determined.

Determination of ξ^*

The dimensionless flame standoff distance ξ^* is given by

$$\xi^* = (m_T c_p/\lambda_g)x^* \tag{29}$$

where x^* is the physical flame standoff distance. It is assumed that a sufficiently accurate value of x^* is given by the product of the average velocity of gases flowing away from the propellant U and the average reaction delay time for a second order, gas phase reaction τ, or $x^* = U\tau$. For the purpose of this simple analysis, we define

$$U = \frac{m_T}{\rho_f} \qquad \text{and} \qquad \tau = \frac{1}{\rho_f Z \exp(-E/RT_f)} \tag{30}$$

where the density ρ_f will be taken as the gas density at the flame temperature. Replacing ρ_f by (gPM_g/JRT_f) and noting that $m_T = \rho_p r$, the dimensionless flame standoff distance in terms of atmospheres of pressure is

$$\xi^* = \beta[Er\theta_f/P]^2 \exp(1/\theta_f) \tag{31}$$

where

$$\beta = \left(\frac{c_p}{\lambda_g Z}\right)\left(\frac{\rho_p J}{1033 \times gM_g}\right)^2 \tag{32}$$

Determination of Q_s

The heat released at the surface of the propellant is equal to the net heat absorbed or released per unit mass by all of

Table 1 "Standard" parameter values for input to theory

Propellant data			
ρ_f	= 1.27 g/cm³ (Polysulphide)	A_f	= 40 cm/sec
ρ_{ap}	= 1.96 g/cm³ (NH_4ClO_4)	Q_{sr}	= 425 cal/g
α	= 0.7	Q_f	= 1200 cal/g
E_f	= 12 kcal/mole	ΔH_p	= 175 cal/g
E_{sr}	= 10.5 kcal/mole	D_{min}	= 163 μ
E	= 45 kcal/mole	D_{max}	= 241 μ
T_0	= 25°C	D_m	= 200 μ
Ammonium perchlorate data			
K_0	= 200 sec-atm^m-cm^{-n}	V	= 0.0384 cm-sec^{-1}-atm$^{-\delta}$
m	= 0.75	δ	= 0.73
n	= 0.8	$(Q_{gp} - Q_L)$	= 320 cal/g

the decompositional processes occurring at the propellant surface. Using the notation of the section on surface processes Q_s is given by

$$Q_s = 1/M_T\ (-\Delta H_p k_f - k_{ox}Q_L + Q_{sr}\cdot k_{sr}(C) + k_{gp}(B)(C)Q_{gp}) \quad (33)$$

Noting that $k_{gp}(B)\ (C) = [k_{ox} - k_{sr}(C)]$, inserting the appropriate mass flux and surface area values of each k, we can write Q_s as

$$Q_s = \alpha(Q_{gp} - Q_L) + \frac{\nu(24)^{1/2}\langle\epsilon/D\rangle}{\rho_p r}(Q_{sr} - Q_{gp})m_{sr} - \frac{(1-\nu)\Delta H_p}{\rho_p r} m_f \quad (34)$$

It must be noted that Q_s is, therefore, a function of the propellant burning rate, the propellant surface temperature, the oxidizer particle diameter, and the ambient pressure level.

Final Equations

At this point, all the necessary relationships have been defined and it is possible to write out, completely, the three algebraic equations relating the three basic unknowns of burning rate, surface temperature, and the flame temperature. However, the condensed form of these equations given below provides a clearer picture of the relationships between the equations:

$$r = a_1 \exp\left(\frac{-E_f}{E\theta_s}\right) + \frac{b_1 P^\delta}{\theta_s^{1/2}}\left[\frac{c_3}{r} - \frac{d_1}{P^m}\right]\cdot\exp\left[\frac{-(E_{ox}+E_{sr})}{E\theta_s}\right] \quad (35)$$

$$\theta_s = b_2 + \left(\frac{b_3 P^\delta}{r\theta_s^{1/2}}\right)\left[\frac{c_3}{r} - \frac{d_1}{P^m}\right]\cdot\exp\left[\frac{-(E_{ox}+E_{sr})}{E\theta_s}\right] - \left(\frac{a_2}{r}\right)\exp\left(\frac{-E_f}{E\theta_s}\right) + a_3\exp\left[-\beta\theta_f^2 e^{1/\theta_f}\left(\frac{r}{P}\right)^2\right] \quad (36)$$

$$\theta_f = \theta_s + a_3\{1 - \exp[-\beta\theta_f^2 e^{1/\theta_f}(r/P)^2]\} \quad (37)$$

where a_1, a_2, a_3, b_1, b_2, b_3, and d_1 are constants (see Nomenclature).

Solution of Equations

Equations (35–37) were solved numerically using an IBM 1620 or 1710 digital computer. The method used in arriving at the results to be discussed was to specify a pressure level, P ($1 \leq P \leq 3200$ atm) and an arbitrary ratio (θ_s/θ_f) for an assumed set of input data (E_f, E_{sr}, E, Q_f, α, ΔD, etc.) and to vary the value of θ_s (calculating the value of r at each θ_s value from Eq. (35)) until Eq. (36) was satisfied. Equation (37) then was checked to see if the selected ratio of (θ_s/θ_f) was compatible with the values of r and θ_s obtained from the previous steps. If the last check revealed an error, the selected ratio of (θ_s/θ_f) was modified by the error revealed by the check; and the whole process was repeated until all three equations were satisfied. The pressure level was changed then and the process was repeated until a set of solutions of r, T_s, T_f, and $\langle\epsilon/D\rangle$ was obtained over a range of pressures for the assumed physical and chemical properties of the propellant. About one and a half minutes were required for the solution at each given pressure level for a selected set of input data, using the IBM 1710.

Selection of Propellant Physical and Chemical Properties

Values for the physical and chemical properties, assumed as input data for the calculations, were determined from available data and by what seemed physically reasonable. The propellant density was calculated for each set of input data.

Parameters for the ignition and combustion of the ammonium perchlorate were obtained from studies of ammonium perchlorate combustion.[8,14] Estimates of the parameter values associated with fuel binder pyrolysis were obtained from Refs. 7, 10, and 11; and estimates of the parameter values for the gas phase combustion process were obtained from Ref. 10. Estimates of ΔD_1 and ΔD_2 for typical particle size distributions in practice were derived from Ref. 4.

Of the propellant burning rate data available to the author, that for a polysulphide (ammonium perchlorate) was reported[3,4] over the widest range of pressures (15–20,000 psia). These data are quite representative of many composite propellants in terms of the effects of pressure, particle size distribution, and oxidizer weight fraction on the burning rate. In particular, the data[3] presented for a polysulphide propellant having a weight fraction of oxidizer of 0.7, with a unimodal particle size distribution and a mean particle diameter of 200, was selected as a standard for comparison with various sets of input data for the theoretical calculations using Eqs. (35–37).

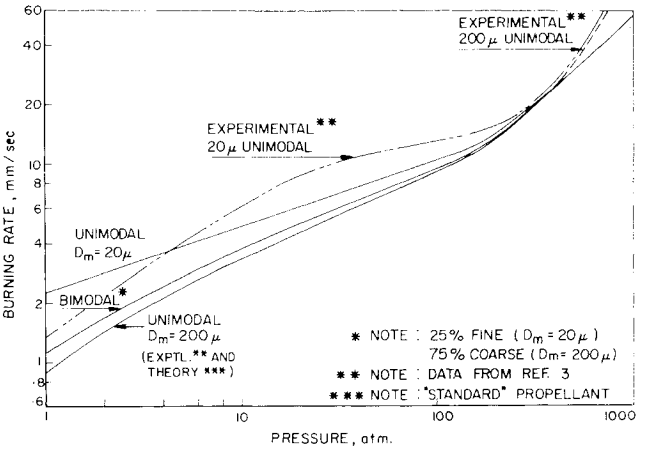

Fig. 3. Comparison of theory with experiment and effect of particle size distribution.

Results and Discussion

It was found that the parameter values given in Table 1 resulted in a remarkably good fit of the standard experimental data, over a pressure range of 1 to 400 atm, and are termed standard for the theoretical calculations reported in this paper. Using this standard set of parameters, many of the properties of the present model are evident in Fig. 3.

Both the present theory and experiment show that the effect of oxidizer particle size on the burning rate becomes negligible at pressures of 200 atm or greater. Evidently the lower pressure burning rates are increasingly affected as the mean particle size of a unimodal oxidizer distribution is reduced; the effect of bimodal distributions lies between that of the equivalent unimodal extremes as seems reasonable.

Agreement between the present model and experiment with respect to the effect of oxidizer particle size is good, at least qualitatively; and the theory incorporates the particle size distribution explicitly, without the use of any concepts which are difficult to visualize.

In addition, the model also predicts the experimentally observed change in the burning rate-pressure curve from a concave down curve to one which is concave up at pressures in excess of 100 atm. This behavior is well documented[3,4] experimentally for a number of different propellant fuel binders and ammonium perchlorate oxidizer. It is thought that the present model of composite propellant combustion

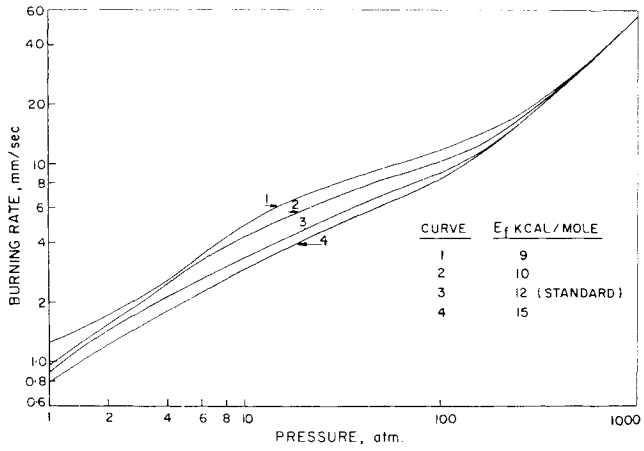

Fig. 4. Influence of the activation energy of fuel binder pyrolysis E_f on the burning rate.

is unique with respect to predicting this high-pressure burning rate behavior.

The increase in burning rate pressure exponent to near unity values is accompanied by a rather sharp increase in propellant surface temperature and decreasing values of the flame standoff distance. However, it may be noted that the theoretical pressure exponent of the burning rate tends toward an asymptotic value, whereas the experimental value continues to increase. Probably equilibrium decomposition of the ammonium perchlorate no longer is possible at pressures above some 400 atm[12]; and possibly another, pressure sensitive, ammonium perchlorate decomposition mechanism takes over. Another possible explanation, assuming the validity of the postulated surface reaction, is that the order of this reaction exceeds unity at sufficiently high surface temperatures, burning rates, and pressure levels. Experimental data on the very high pressure burning rate characteristics of composite propellants having oxidizers other than ammonium perchlorate would be most interesting in this regard.

Influence of Activation Energies E_f, E_{sr}, and E

Figure 4 shows the calculated (r-P) curves for several values of the fuel pyrolysis activation energy E_f. As one might expect, decreasing E_f increased the burning rate at a given pressure level, except at high pressures burning rates, where the surface temperatures were sufficiently high to make the effect of E_f variations negligible. Interestingly enough, it was found that the calculated surface temperatures tended to increase as E_f was decreased; in the pressure range where different E_f values had little effect on the burning rate, the surface temperatures were quite unaffected also by the E_f value. It may be noted that E_f variations affected the burning rate over the entire pressure range of practical interest.

Increases in the fuel binder pyrolysis pre-exponential factor A_f caused results that were equivalent to increases in E_f, and vice versa, in terms of the calculated values of r, T_s, and T_f, and no data therefore is presented.

It is apparent from Fig. 5 that variations in the activation energy of the surface reaction E_{sr} affected the burning rate somewhat differently than did changes in E_f, having the greatest effect at intermediate pressures and little at high pressures. Decreasing values of E_{sr} (and therefore increased values of m_{sr}) caused the burning rate to increase; but in this case, the surface temperatures decreased when E_{sr} was decreased, although the change in T_s was about 55°C at most for E_{sr} values between 9.5 and 15 kcal/mole. In view of Eqs. (23, 34, and 35), this behavior is not surprising when the heat released by the surface reaction Q_{sr} is less than that available from the gas phase combustion of the oxidizer Q_{op}. Physically, this means that the oxidant C produced by the oxidizer decomposition is consumed more readily in the surface reaction than in the gas phase oxidizer decomposition step.

Variations in the value of the activation energy for the propellant gas phase combustion process E were found to affect the high pressure behavior of the burning rate alone (see Fig. 6), since by Eqs. 29–32, E determines the flame standoff distance (x^*) and the heat feedback to the propellant surface. Consequently, E variations have their largest effect where the (E/p^2) term in Eq. (30) becomes small, making x^* decrease rapidly. Finally, it may be noted that variations in the pre-exponential factor Z of the gas phase reaction produce effects similar to equivalent changes in E, and therefore no data is reported.

The Effect of Q_{sr} and H_p

Figure 7 indicates the quite sensitive dependence of the predicted burning rate behavior on the value assumed for the surface reaction heat release Q_{sr}. The predicted surface temperatures are equally sensitive to Q_{sr} and change in the same direction. The general effect of Q_{sr} could be anticipated from Eq. (33). Nevertheless, the evident sensitivity of the results to the selection of Q_{sr} is admittedly surprising, but it is a consequence of the combustion mechanism postulated in this paper and must be accepted as such. It represents an area requiring further study.

The value of Q_{sr} in Table 1 was selected purely by fitting the calculated (r-P) curve to the standard experimental data[3]

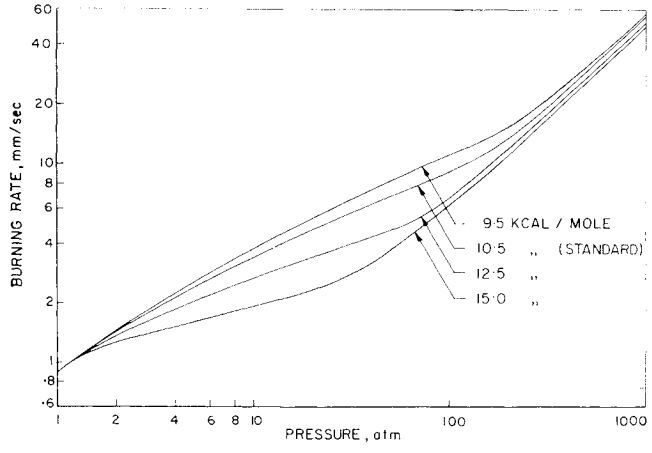

Fig. 5 Effect of the activation energy of the surface reaction E_{sr} on the burning rate.

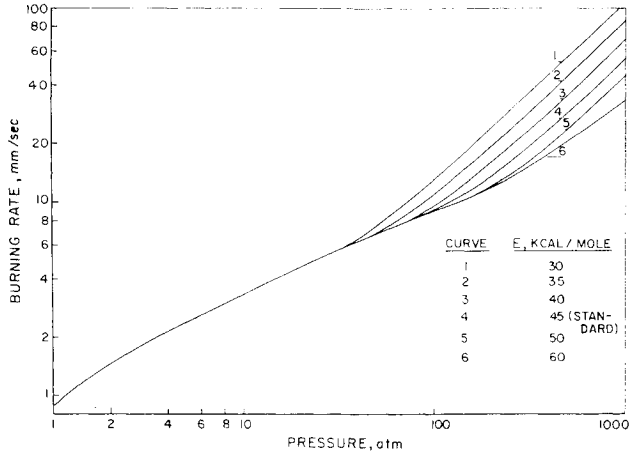

Fig. 6 Influence of the activation energy of the gas phase reaction E on the burning rate.

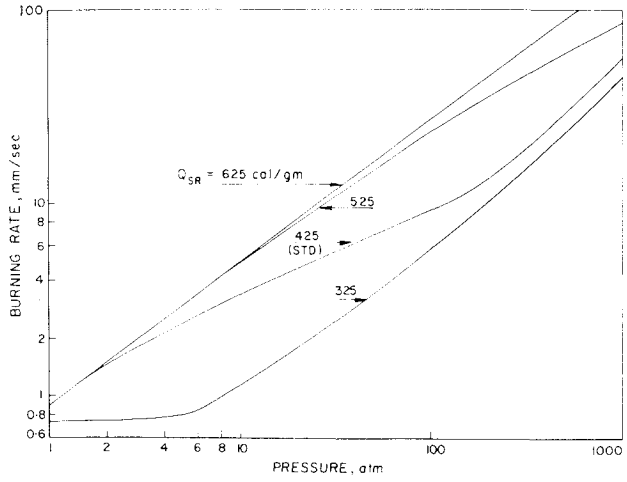

Fig. 7 Effect of various values of the heat released by the surface reaction Q_{sr} on the burning rate.

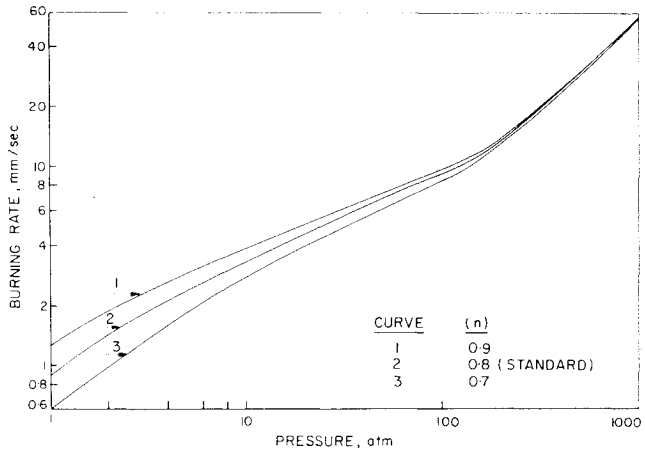

Fig. 9 Effect of exponent (n) of the oxidizer particle diameter in the particle ignition term on the propellant burning rate.

mentioned previously, and is about one fourth of the heat released by the heterogeneous C (graphite) $+ \frac{1}{2}\ O_2(g) \rightarrow CO(g)$ reaction.

The influence of the value assumed for the endothermicity[15] of the fuel binder pyrolysis ΔH_p also was investigated for a range of values between 0 and 250 cal/g. It was found that the effect was most noticeable in the pressure range from 50 to 100 atm. However, the magnitude of the changes in the resultant (r-P) curves and surface temperatures was less than 5% at most, and no graphs were drawn.

Effect of Changing Ignition and Burning Rate Parameters of Ammonium Perchlorate

Variations in the parameters K_0, m, and n alter the ignition delay of the individual oxidizer crystals and affect the calculated (r-P) curves in an informative manner. Changes in the ignition constant K_0 and in the sensitivity of the ignition process to the crystal diameter have very noticeable effects (see Figs. 8 and 9). Changes in (K_0) and (n) are, according to Eq. (14c), equivalent to changes in the mean crystal diameter; this is evident by comparing Figs. 3, 8, and 9. Changes in the pressure sensitivity of the crystal ignition have a minor, relatively constant effect on the r-P curve over the pressure range 6–100 atm of +6% for $m = 0.85$ and −8% for $m = 0.65$. Decreases in K_0 and n result in greatly increased low pressure burning rates and lower surface temperatures. Thus, the model indicates that low pressure propellant burning rates can be controlled over quite wide ranges by the addition of appropriate catalysts affecting the oxidizer ignition process.

The parameters V and δ affect the linear burning rate of the oxidizer crystals [see Eq. (14c)].§ The linear rate constant V has a small effect on the (r-P) curve, most noticeably in the intermediate pressure range of 10–200 atm, with a maximum effect at 100 atm. At this pressure, $V = 0.05$ produced an r change of +6%; whereas $V = 0.025$ produced an r change of −15% from the standard (r-P) curve with $V = 0.0384$. Variations in the pressure sensitivity (δ) of the oxidizer burning rate had little effect on the (r-P) curve at low pressures, but had an increasing effect as the pressure increased (see Fig. 10); δ was the only "physical" parameter that had any strong effect on the (r-P) curve at high pressures.

The results discussed thus far indicate the following picture of the combustion process: at low pressures, oxidizer crystal ignition is controlling, the heterogeneous reaction is dominant at intermediate pressures, whereas at high pressures, the gas phase flame position controls the over-all combustion process.

Effect of Propellant Initial Temperatures and Oxidizer Weight Fraction

Figure 11 contains calculated (r-P) curves for the standard data but various assumed values of the initial propellant temperature T_0. Although the trends evident in this figure

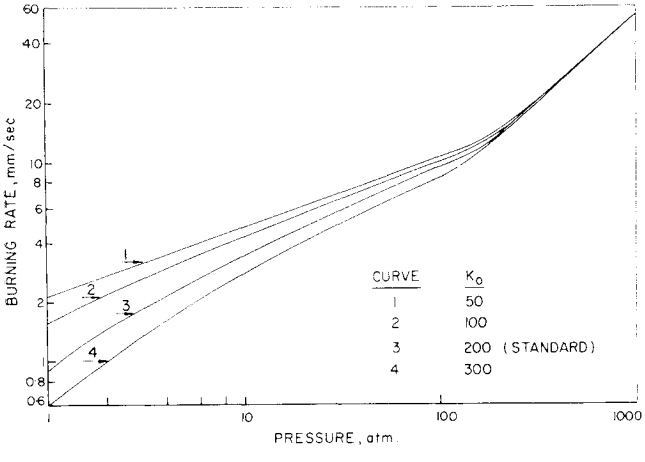

Fig. 8 Influence of the oxidizer ignition parameter K_0 on the propellant burning rate.

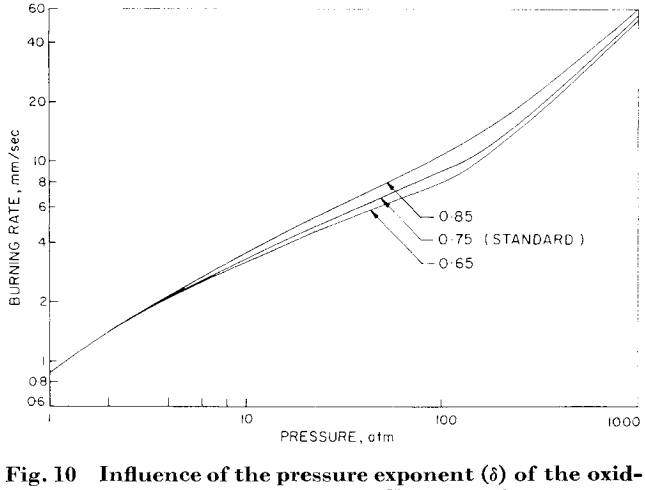

Fig. 10 Influence of the pressure exponent (δ) of the oxidizer burning rate on the propellant burning rate.

§ Both of these parameters can depend on the nature of the fuel binders decomposition products surrounding the oxidizer crystals.[14]

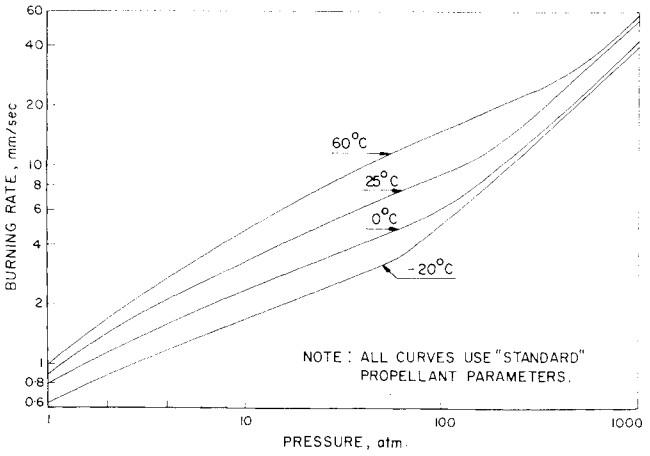

Fig. 11 Effect of initial propellant temperature T_0 on the propellant burning rate.

are clearly correct, the magnitude of the predicted changes in burning rate are about 15% per 10°C change in initial temperature. Typical experimental results[16] are about 5% per 10°C, indicating that the model is not satisfactory in this respect.

The applicability of the proposed model for predicting the effect of varying the oxidizer weight fraction on the propellant burning rate may be seen from Fig. 12 for a standard propellant, but with a unimodal particle size distribution having a diameter of 20 μ. This particle diameter was selected to facilitate comparison of the theoretical results with the data of Bastress.[4] Although the predicted results are in basic accord with experience, comparison of Fig. 12 with the results shown in Fig. 14 of Ref. 4 indicates only the most qualitative agreement between theory and experiment. Consequently, the proposed model also is somewhat deficient in this respect.

Predicted Values of T_s, Q_s, and $\langle \epsilon/D \rangle$

The predictions of the model concerning the magnitude and behavior of the propellant surface temperature T_s were one of the most interesting results of the calculations; see Fig. 13 for a plot of T_s vs pressure level for unimodal propellants having mean particle diameters of 200 μ, 20 μ, and 9 μ, and a bimodal propellant with a (75/25) split of 200 μ and 20 μ particles. The predicted value of T_s for a 9 μ particle size (but otherwise standard) propellant is approximately 625°C $\pm$ 10°C between 1 and 100 atm. This is in good agreement with the measured values of 600° $\pm$ 50°C for a 9 μ mean

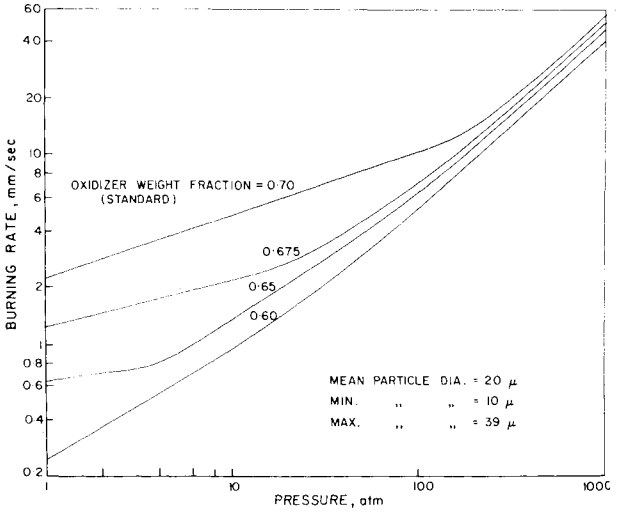

Fig. 12 Effect of oxidizer weight fraction of propellant for a constant, unimodal oxidizer particle size distribution.

diameter, 70% oxidizer, unimodal propellant over a pressure range from 1 to 10 atm.[5] The fact that the predicted values of T_s, for the standard propellant with a 9 μ mean diameter particle size, varied little with the pressure level also is in good agreement with measurement.[5]

From these experimental results,[5] the existence of a heat release near (or at) the propellant surface amounting to some 130 cal/g of propellant burned was deduced. For the 9 μ particle diameter, but otherwise standard propellant, the predicted value of the heat release at the surface was approximately 165 cal/g of propellant burned, which is reasonably compatible with the experimental value just mentioned. Values of Q_s for other particle diameters can be calculated easily from the data given in the figures and in Eqs. 17, 23, and 34, but for lack of space they are not quoted here.

The behavior of $\langle \epsilon/D \rangle$ (the over-all ratio of the depth of fissure surrounding an oxidizer crystal to the diameter of the crystal) vs pressure, is shown in Fig. 14 for two different unimodal particle size distributions. It may be noted that a maximum value of $\langle \epsilon/D \rangle$ is attained at about 200 atm, after which the ratio decreases. Physically, Fig. 14 shows that at low pressures the oxidizer particles protrude above the surface of the surrounding fuel matrix. As the pressure increases, the degree of crystal protrusion decreases until the crystals are level with (or below) the fuel surface. At pressures above about 200 atm, this process reverses as the burning rates become very large. This behavior of the oxidizer crystals is in very good agreement with the observations reported by Bastress.[4]

Flame Standoff Distance

From the computed values of r, T_f, and the value of β used in the calculations, it is possible to compute the value of the flame standoff distance predicted by the solution of Eqs. (35–37), by using Eqs. (29) and (31). The standard propellant data result in the formula $x^* = (50r/P^2)$ cm, from which the computations show an x^* ranging from 5 cm at 1 atm and a 1 mm/sec burning rate to 50 μ at 100 atm, and a 1 cm/sec burning rate. Quite clearly, the proposed model gives rather unrealistic values for the flame standoff distance.

Conclusions

The preceeding discussion of the predictions about the combustion of composite propellants, resulting from the analysis of the proposed model, has revealed the areas of agreement and disagreement with available experimental data.

Summing up, there is little or no evidence which unequivocally indicates the existence of the heterogeneous reaction which is postulated to occur around the oxidizer crystals and which is an important aspect of the proposed model.¶ The results of the model are quite sensitive also to the assump-

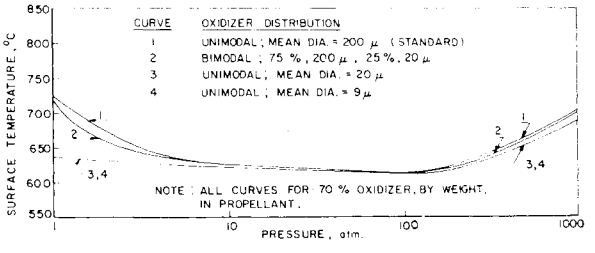

Fig. 13 Predicted propellant surface temperatures for several particle size distributions.

¶ Recent experiments[17] have, however, demonstrated that several common composite propellant fuel binders can be ignited at 300°C (1 atm) by 72% $HClO_4$ vapor, but the mechanism of ignition and combustion is still unknown.

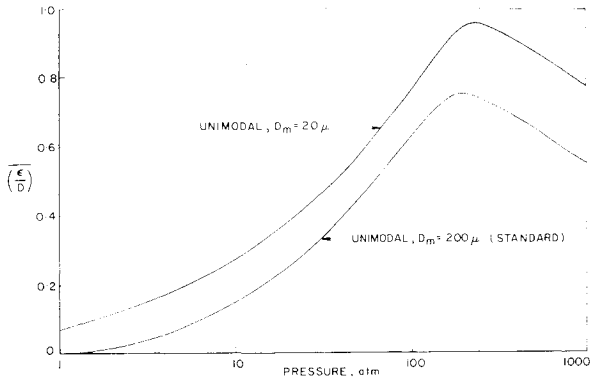

Fig. 14 Ratio of surface reaction depth (ϵ) to particle diameter (D) as a function of pressure level.

tions made about the magnitude of the heat released by this reaction. In addition, the model ignores the diffusion processes in the gas phase which should be important, at least at high pressures. Predictions of the effect of oxidizer weight fraction are also at variance with experimental data, although the effects of experimental uncertainties in the value of parameters involved in the ignition and linear burning rate of the oxidizer were found to be small. The model is somewhat overly sensitive to the value of initial propellant temperature, and finally, it predicts rather unreasonable values of the flame standoff distance, particularly at low pressures. Efforts to improve the model in these aspects are currently underway and will be reported in the future.

On the favorable side, however, there is quite good agreement between theory and experiment concerning the burning rate-pressure relationship over a wide pressure range. The effect of various particle size distributions is predicted in a correct manner, at least qualitatively. The model incorporates the particle size distribution explicitly, with little if any artificiality, and uses reported data concerning the oxidizer combustion. Good agreement exists between the derived and experimentally observed behavior of the oxidizer crystals with respect to the fuel binder surface over a wide range of pressure and particle sizes. Finally, the model predicts a magnitude and behavior of the temperature of the burning surface of the propellant which is in good agreement with experimental data as well as a very reasonable value for the heat generated in the region of the burning surface.

Considering the simple mathematical structure of the analysis and the existing degree of agreement between the theory and experiment, the assumed physical model may be a step in the right direction toward obtaining the correct picture of the combustion process of composite solid propellants.

References

[1] Nachbar, W., "A theoretical study of the burning of a solid propellant sandwich," *ARS Progress in Astronautics and Rocketry: Solid Propellant Rocket Research*, edited by M. Summerfield (Academic Press Inc., New York, 1960), Vol. I, pp. 207–226.

[2] Summerfield, M., Sutherland, G., Webb, M., Taback, H., and Hall, K. P., "Burning mechanism of ammonium perchlorate propellants," *ARS Progress in Astronautics and Rocketry: Solid Propellant Rocket Research*, edited by M. Summerfield (Academic Press Inc., New York, 1960), Vol. I, pp. 141–182.

[3] Summerfield, M., Wenograd, J., Cole, R. B., and Hall, K. P., "Burning rate control factors in solid propellants," 11th and 12th Quarterly Technical Summary Reports (1961); also Princeton Univ., Aeronautical Engineering Rept. 446, K and L (March 1962).

[4] Bastress, E. K., "Modification of the burning rates of ammonium perchlorate propellants by particle size control," Princeton Univ., Ph.D. Thesis, Aeronautical Engineering Rept. 536 (March 1961).

[5] Sabadell, A. J., Wenograd, J., and Summerfield, M., "Measurement of temperature profiles through solid-propellant flames using fine thermocouples," AIAA J. **3**, 1580–1584 (1965).

[6] McAlevy, R. F. and Hansel, J. G., "Linear pyrolysis of thermoplastics in chemically reactive environments," AIAA J. **3**, 244–249 (1965).

[7] Anderson, R. and Brown, R., "Fundamental theory of hypergolic ignition for solid propellants," AIAA Preprint 63-514 (December 1963).

[8] Petersen, E. E. and Shannon, L. J., "Deflagration characteristics of ammonium perchlorate strands," AIAA J. **2**, 168–169 (1964).

[9] Marklund, T., "Ignition of ammonium perchlorate as a function of pressure level," Paper presented at Annual Meeting of Combustion Section of Swedish Academy of Sciences, the Royal Institute of Technology, Stockholm (November 1964).

[10] Benson, S. W., *The Foundations of Chemical Kinetics* (McGraw-Hill Book Company Inc., New York, 1960), Chap. XVII.

[11] Frank-Kamenetskii, D. A., *Diffusion and Heat Exchange in Chemical Kinetics* (Princeton University Press, Princeton, N. J., 1955), pp. 58–59.

[12] Powling, J. and Smith, W. A. W., "The surface temperature of burning ammonium perchlorate," Combust. Flame **7**, 269–275 (1963).

[13] Inami, S. H., Rosser, W. A., and Wise, H., "Dissociation pressure of ammonium perchlorate," J. Phys. Chem. **67**, 1077–1079 (1963).

[14] Barrere, M. and Nadaud, L., "Combustion of ammonium perchlorate spheres in a flowing, gaseous fuel," *Tenth Symposium (International) on Combustion* (The Combustion Institute, Pittsburgh, Pa., 1965), pp. 1381–1394.

[15] Rabinovitch, B., "Regression rates and kinetics of polymer degradation," *Tenth Symposium (International) on Combustion* (The Combustion Institute, Pittsburgh, Pa., 1965), pp. 1395–1404.

[16] Hugget, C., Bartley, C. E., and Mills, M. M., *Solid Propellant Rockets*, edited by C. D. Donaldson (Princeton Aeronautical Paperbacks, Princeton University Press, Princeton, N. J., 1960), p. 33.

[17] Pearson, G. S. and Sutton, D., "Ignition of composite propellant fuels by perchloric acid vapor," AIAA J. **41**, 954–955 (1966).